NATIONAL ADVISORY COMMITTEE FOR AERONAUTICS

TECHNICAL NOTE 3320

FLIGHT MEASUREMENTS OF DRAG AND BASE PRESSURE OF A FIN-STABILIZED PARABOLIC BODY OF REVOLUTION (NACA RM-10) AT DIFFERENT REYNOLDS NUMBERS AND AT MACH NUMBERS FROM 0.9 TO 3.3

By H. Herbert Jackson, Charles B. Rumsey, and Leo T. Chauvin

Langley Aeronautical Laboratory
Langley Field, Va.

Washington
November 1954

S

NATIONAL ADVISORY COMMITTEE FOR AERONAUTICS

TECHNICAL NOTE 3320

FLIGHT MEASUREMENTS OF DRAG AND BASE PRESSURE OF A FIN-STABILIZED PARABOLIC BODY OF REVOLUTION (NACA RM-10) AT DIFFERENT REYNOLDS NUMBERS AND AT MACH NUMBERS FROM 0.9 TO 3.3[1]

By H. Herbert Jackson, Charles B. Rumsey, and Leo T. Chauvin

SUMMARY

Free-flight tests have been made to investigate the total drag and base drag at different Reynolds numbers of full-scale and half-scale models of an NACA research model designated the RM-10. The general shape of the body was a parabola of revolution of fineness ratio 12.2 with a blunt base to provide space for the rocket jet. The models were stabilized by four 60° sweptback fins mounted at the base of the bodies.

The Mach number range of the tests was approximately 0.9 to 3.3. The ranges of Reynolds number, based on body length, were from 14×10^6 to 210×10^6 for the full-scale models and 15×10^6 to 110×10^6 for the half-scale models.

The results show that the total drag coefficients for both models reached a maximum at transonic speed and gradually decreased over the entire supersonic range, whereas the base drags were a maximum at transonic speeds and a minimum at about Mach number 1.2 for the supersonic speed range.

It is indicated that there was, at most, only a small effect on the total drag coefficient of the configuration at a given Mach number due specifically to reductions in Reynolds number of 20×10^6 to 120×10^6 over the Reynolds number range from 40×10^6 to 210×10^6. The base-drag coefficient of the half-scale models was 25 to 50 percent lower

[1]Supersedes the recently declassified NACA RM L50G24, "Flight Measurements of Drag and Base Pressure of a Fin-Stabilized Parabolic Body of Revolution (NACA RM-10) at Different Reynolds Numbers and at Mach Numbers From 0.9 to 3.3" by H. Herbert Jackson, Charles B. Rumsey, and Leo T. Chauvin, 1950.

than that of the full-scale model. The difference in base-drag coefficient would account for practically all the difference in the total drag coefficient of the two models; hence, there is small effect of Reynolds number changes at a given Mach number on forebody drag coefficient over the Reynolds number range of the tests. This small effect would be expected from the present knowledge of skin friction in this Reynolds number range. The difference in base-drag coefficient was possibly due to either the difference in Reynolds number at a given Mach number or to differences in the internal base configuration between the full-scale and half-scale models. Part of the decrease in total drag coefficient with increasing Mach number over the higher portion of the Mach number range was doubtless due to the reduction of skin-friction coefficient with increasing Mach number.

INTRODUCTION

As part of a program of supersonic research by the National Advisory Committee for Aeronautics, the Langley Pilotless Aircraft Research Division has made a series of flight tests at its Pilotless Aircraft Research Station at Wallops Island, Va., to investigate the drag at different Reynolds numbers of a fin-stabilized parabolic-arc body of revolution designated the NACA RM-10. This investigation is part of a coordinated program including also tests of the same configuration in various wind tunnels in order to assess the effects of Reynolds number on drag characteristics. Data from the Lewis 8- by 6-foot supersonic tunnel are given in reference 1. The change of Reynolds number in the present tests was obtained by using models of identical configuration but of different scale and by boosting the models to obtain various altitude-velocity relationships.

Reported herein are zero-lift total-drag data for nine models of the same configuration. Base-drag data were obtained on five of these models. Five of the models were half the scale of the other four, which are designated full-scale models. Some of the models were used concurrently for investigation of heat-transfer and boundary-layer phenomena at high Reynolds numbers in supersonic flow.

The Mach number range of the data presented is from approximately 0.85 to 3.30 for the full-scale models and 0.90 to 3.02 for the half-scale models. The Reynolds number ranges were from 14×10^6 to 210×10^6 for the full-scale models and 15×10^6 to 110×10^6 for the half-scale models. These Reynolds numbers are based on body length.

SYMBOLS

C_D	drag coefficient
C_{D_T}	total drag coefficient, based on maximum cross-sectional area of the body (0.785 sq ft for full scale and 0.196 sq ft for half scale)
C_{D_B}	base-drag coefficient, based on maximum cross-sectional area of the body
D	diameter, in.
M	Mach number
M_{max}	maximum Mach number
p_b	base pressure, lb/sq ft
p_o	ambient static pressure, lb/sq ft
$\frac{\Delta p}{q}_{base}$	base-pressure coefficient, $\frac{p_b - p_o}{q}$
q	dynamic pressure, lb/sq ft
R	Reynolds number, based on body length (12.2 ft for full scale and 6.1 ft for half scale)
t/c	thickness ratio

MODELS AND TESTS

The general configuration and body equations of the test models are given in figure 1. A photograph of the full-scale model is shown in figure 2 and photographs of both the full-scale and half-scale models in launching position are shown in figure 3.

The bodies had a parabolic-arc profile with the basic parabolic shape having a fineness ratio of 15. Cutting off the pointed stern at 81.25 percent of the full length to allow space for the rocket jet resulted in an actual body fineness ratio of 12.2. The four stabilizing fins were equally spaced around the stern. Their plan form was untapered

and sweptback 60° with a total aspect ratio of 2.04. They had a 10-percent-thick circular-arc cross section normal to the leading edge. The thickness ratio in the streamwise direction was 5 percent.

The full-scale model had a body length of 12.2 feet and a frontal area, on which the drag coefficients are based, of 0.785 square foot. The half-scale model had a length of 6.1 feet and a frontal area of 0.196 square foot.

The bodies of the models were constructed with spun magnesium-alloy skins and the tail cones, to which the fins were attached, were constructed with cast magnesium alloy.

All models carried internally a sustainer motor; one full-scale and all half-scale models also utilized various booster rocket motors to obtain high Mach numbers. The rocket motors used and maximum Mach numbers reached are given in the following table:

Models	Sustainer rocket motor	Total impulse, lb-sec	Booster rocket motor	Total impulse, lb-sec	M_{max}
Full-scale - 1,2,3	6.25-inch ABL Deacon used in all models	19,800	----------	--------	2.7
Full-scale - 4			6.25-inch ABL Deacon	19,800	3.45
Half-scale - A	Modified 3.25-inch Mark 7 used in all models	1,720	3.25-inch Mark 7	1,720	1.6
Half-scale - B			5-inch HVAR lightweight	4,900	2.1
Half-scale - C,D,E			6.25-inch ABL Deacon	19,800	3.1

The variation of Reynolds number with Mach number obtained in the tests is shown in figure 4. Two curves are shown to represent the relation between the Mach number and the Reynolds number for the full-scale models; one depicts the variation for the unboosted models 1, 2, and 3, and the second shows the variation for the boosted model 4. There are three curves shown for the half-scale models since each of the three types of booster rockets used resulted in a different altitude-velocity relation during flight. As can be seen, for a given Mach number the test Reynolds numbers of the unboosted full-scale models were approximately twice those of the half-scale models, whereas for the boosted full-scale model the Reynolds numbers were roughly equivalent to those of the half-scale models.

Data were reduced for the decelerating portion of the flight trajectory after rocket-motor burnout. Trajectory and atmospheric data were obtained from the NACA modified SCR 584 radar tracking unit and by radiosonde observations. Velocity and total drag were obtained from the CW Doppler radar set as described in reference 2. Also, total drag and base drag were reduced from data telemetered to a ground receiving station by instrumentation incorporating a longitudinal accelerometer and a pressure cell.

Base pressure was measured inside the afterbody between the rocket nozzle and the skin by an open-ended tube located in the full-scale and half-scale models as shown in figures 5 and 6. The annular area around the rocket motor at the base was sealed from the forward part of the body to prevent internal air flow. The base-drag coefficient was computed as equal to the product of the base-pressure coefficient and the ratio of the base area to the body frontal area, which is 0.367. This computation assumes that the measured base pressure acts over the entire area of the base.

ACCURACY

Total drag coefficient.- The random scatter of the data points for the total drag coefficient for any one model is very small, as can be seen in figures 7 and 8, even though some difference is apparent between the results of different models of the same scale. The results of models of the same scale do, however, determine a mean curve of total drag coefficient from which the maximum discrepancy in total drag coefficient at any supersonic Mach number is ± 0.008 or approximately ± 3.5 percent for the full-scale models and ± 0.015 or approximately ± 6.5 percent for the half-scale models. The accuracy of the mean curves is, however, believed to be much greater than these maximum discrepancies; the accuracy is probably around ± 0.005 over the supersonic speeds for both the full-scale and half-scale models. In the transonic and subsonic speeds the accuracy is somewhat less, probably about ± 0.01.

Base-pressure and base-drag coefficients.- The frequency response (ratio of recorded pressure to actual pressure) of the base-pressure measuring system, from the end of the base-pressure tube through the pressure instrument, was 1 up to frequencies of approximately 3 cycles per second and 5 cycles per second for the full-scale and half-scale models, respectively. Since the only oscillation in base pressure was that which occurred through the transonic speed range and had a frequency of approximately 1/5 cycle per second, these relatively low frequency responses were satisfactory. The time-lag constant for the pressure system of both models was less than 0.0007 second. At the lower Mach numbers investigated, the base-pressure coefficients are subject to

rather high systematic errors, since the quantity $(p_b - p_o)$ is of the same order of magnitude as the reliability of the telemetered base-pressure measurements. Although the systematic errors in $\left(\frac{\Delta p}{q}\right)_{base}$ may be large, the scatter of the data indicates that for transonic speeds a probable accuracy of ± 0.03 in $\left(\frac{\Delta p}{q}\right)_{base}$ or, because of the area-ratio factor, an accuracy of ± 0.01 in C_{D_B}. The probable accuracy of C_{D_B} at $M = 2.5$ is ± 0.003.

Model contours.- The body coordinates of the test models were within 0.020 inch of the design values and the surfaces were smooth and highly polished at the time of launching. Changes in surface conditions due to heating during flight are believed to have been small since the design of the models is such as to hold irregular expansions to a minimum.

RESULTS AND DISCUSSION

Drag results for the full-scale and half-scale models are presented over Mach number ranges of 0.85 to 3.30 and 0.90 to 3.02, respectively, in figures 7 and 8. Both total drag coefficient C_{D_T} and base-drag coefficient C_{D_B} are based on the maximum body frontal areas.

Total drag coefficient C_{D_T} as obtained from the CW Doppler radar set is shown to as low a Mach number (that is, distance out) as was covered by that instrument. At lower Mach numbers C_{D_T} was determined from telemetered drag-accelerometer data except for full-scale model 2 and half-scale models C and D which experienced telemeter failures.

Good agreement in total drag coefficient is shown in figure 7 between the boosted and unboosted full-scale models. This agreement in C_{D_T}, obtained in tests of greatly different Reynolds numbers, indicates that the effects of Reynolds number change at a given Mach number on the drag of this configuration are small over the range 40×10^6 to 210×10^6. The fact that the effect is small is also indicated by the agreement in C_{D_T} of the half-scale models whose Reynolds numbers at a given Mach number were also somewhat different. The mean C_{D_T} curve for the full-scale models shows a maximum C_{D_T} of 0.26 at Mach number 1.04; the curve gradually decreases to 0.21 at Mach number 2.5 and then decreases more rapidly to 0.17 at Mach number 3.3. The mean curve for the half-scale models shows a maximum C_{D_T} of 0.25 at Mach number 1.05; the curve

gradually decreases to 0.19 at Mach number 3.0. Measurements of boundary-layer characteristics made on the full-scale configuration also show a significant decrease in friction-drag coefficient with increasing supersonic Mach number. (See ref. 3.)

The curve of the base-drag coefficient C_{D_B} for the full-scale models, presented in figure 7, was computed from base-pressure measurements made on only one model. The base-drag coefficients as determined from half-scale models A, C, D, and E determine a mean curve which shows roughly the same characteristics, although the values are lower than those of the single full-scale model. Both show a maximum coefficient in the transonic range and a minimum at about Mach number 1.2 for the supersonic speed range. As can be seen from the curves, the C_{D_B} for the full-scale model has an average value of approximately 0.04 and the half-scale mean curve has an average value of approximately 0.025. The differences in C_{D_B} may be due to a combination of three things: the difference in Reynolds number at a given Mach number, the difference in internal base configurations, and the afterburning effects characteristic of the sustainer rocker motors used in the models. As can be seen from figures 5 and 6, the internal volume from the base forward to the base-pressure measurement tube contained between the rocket motor and the skin is as much as seven times as great, relatively, in the full-scale models as in the half-scale models. Unpublished data have shown that the 3.25-inch Mark 7 sustainer rocket motor used in the half-scale models may have sufficient afterburning to cause noticeable reductions in base-drag coefficients. It has been observed that this afterburning may act in a manner similar to that of a base bleed. Because of this possible afterburning of the 3.25-inch Mark 7 rocket motor, it is believed that the base-drag coefficient obtained from the full-scale model is more representative of the true base drag.

The measured base-pressure coefficient $\left(\frac{\Delta p}{q}\right)_{base}$ from which C_{D_B} was calculated is shown for both full-scale and half-scale models in figure 9 along with a calculated curve of $\left(\frac{\Delta p}{q}\right)_{base}$ for full-vacuum base pressure. Also shown in figure 9, for ease of comparison, are the Reynolds numbers at which the data for the base-pressure coefficients were obtained.

For comparison of the results obtained at different Reynolds numbers, arbitrarily averaged curves of total drag and base-drag coefficients for both the full-scale and half-scale models are shown in figure 10. It can be seen that the curves of the total drag coefficient for both models are similar; however, the full-scale curve is higher than that of the half-scale models by approximately 0.015 over the supersonic range to Mach number 2.5. Beyond Mach number 2.5, the two curves

approach each other and reach the same value of C_{D_T}, 0.195, at Mach number 2.9. A comparison of the base-drag curves again shows the full-scale values to be higher by roughly 0.015 over the measured range and also shows that the curves tend to converge at higher Mach numbers.

Subtracting the base-drag curve from the total-drag curve for both groups of models yields curves of total drag of the forebody, including fins. The comparison in figure 11 of these curves shows that they are in good agreement and indicate, at most, only small effect on the forebody drag due to the Reynolds number difference between the full-scale and half-scale tests over the range of Reynolds numbers covered. This agreement might be expected from the compensating character of the two probable major Reynolds number effects on body drag, that is, a larger percentage of laminar boundary layer on the half-scale models and a lower average turbulent skin-friction coefficient on the full-scale body due to its higher Reynolds numbers. Since the components making up forebody-plus-fin drag were not measured individually, it was impossible to determine the effects, if any, of Reynolds number change on these components.

CONCLUSIONS

The supersonic zero-lift drag of a parabolic body configuration has been measured on both full-scale and half-scale models. The test Reynolds numbers of the unboosted full-scale models were approximately twice those of the half-scale models; whereas for the boosted full-scale model, the Reynolds numbers were roughly equivalent to those of the half-scale models. Within the limits of the investigation, the results indicated the following:

1. The total-drag coefficient for both models reached a maximum at transonic speed and gradually decreased over the entire supersonic range, whereas the base drags were a maximum at transonic speeds and a minimum at about Mach number 1.2 for the supersonic speed range with relatively constant values over the rest of the supersonic range.

2. There is, at most, only small effect on total-drag coefficient of the NACA RM-10 configuration at a given Mach number due specifically to reductions in Reynolds number, based on body length, of 20×10^6 to 120×10^6 over the Reynolds number range from 40×10^6 to 210×10^6.

3. The base-drag coefficient of the half-scale models was 25 to 50 percent lower than that of the full-scale model. This difference may be due to a combination of three things: the difference in Reynolds number at a given Mach number, the difference in the internal base configurations between the full-scale and half-scale models, and the afterburning

effects characteristic of the sustainer rocket motors used in the models. It is believed that, because of possible afterburning effects on the base drag of the half-scale model, the base-drag coefficient of the full-scale model is more representative of the true base drag.

4. The difference in base-drag coefficients would account for practically all the difference in the total drag coefficients of the two models; thus, effect of Reynolds number change on the forebody drag coefficient at a given Mach number is small in the Reynolds number range of these tests.

Langley Aeronautical Laboratory,
National Advisory Committee for Aeronautics,
Langley Field, Va., August 4, 1950.

REFERENCES

1. Luidens, Roger W., and Simon, Paul C.: Aerodynamic Characteristics of NACA RM-10 Missile in 8- by 6-Foot Supersonic Wind Tunnel at Mach Numbers From 1.49 and 1.98. I - Presentation and Analysis of Pressure Measurements (Stabilizing Fins Removed). NACA RM E50D10, 1950.

2. Morrow, John D., and Katz, Ellis: Flight Investigation at Mach Numbers From 0.6 to 1.7 To Determine Drag and Base Pressures on a Blunt-Trailing-Edge Airfoil and Drag of Diamond and Circular-Arc Airfoils at Zero Lift. NACA RM L50E19a, 1950.

3. Rumsey, Charles B., and Loposer, J. Dan: Average Skin-Friction Coefficients From Boundary-Layer Measurements in Flight on a Parabolic Body of Revolution (NACA RM-10) at Supersonic Speeds and at Large Reynolds Numbers. NACA RM L51B12, 1951.

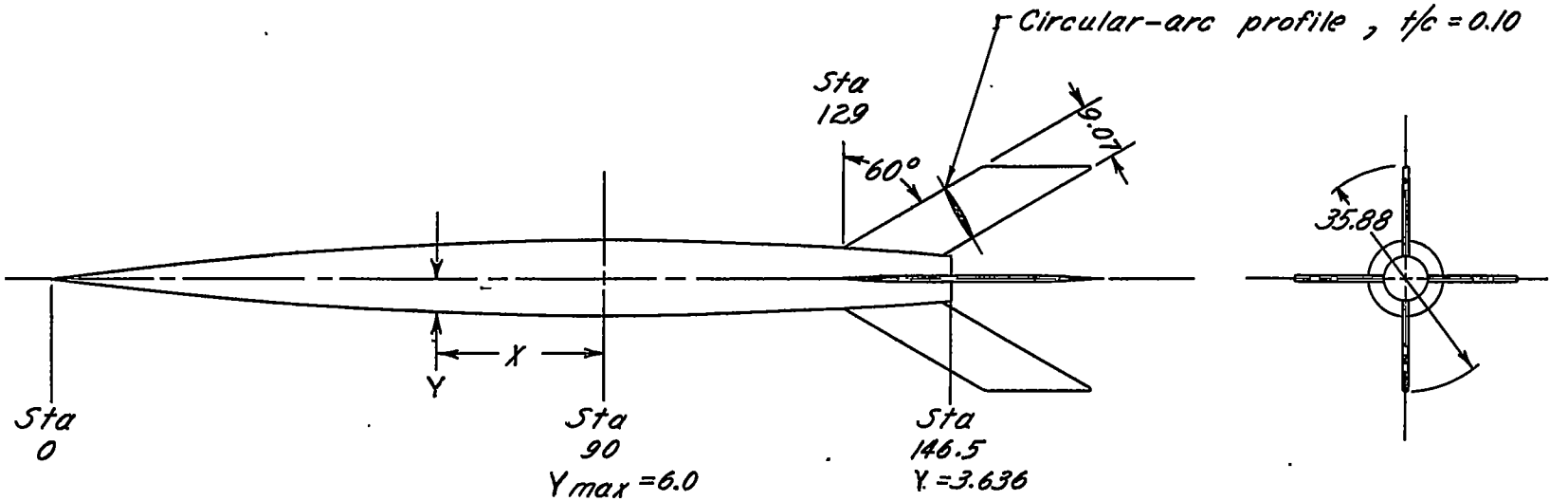

Full-scale model

Body profile equations:
Full-scale body , $Y = 6.000 - .0007407\,X^2$
Half-scale body , $Y = 3.000 - .0014814\,X^2$

Figure 1.- General configuration of RM-10 test models. Dimensions are in inches.

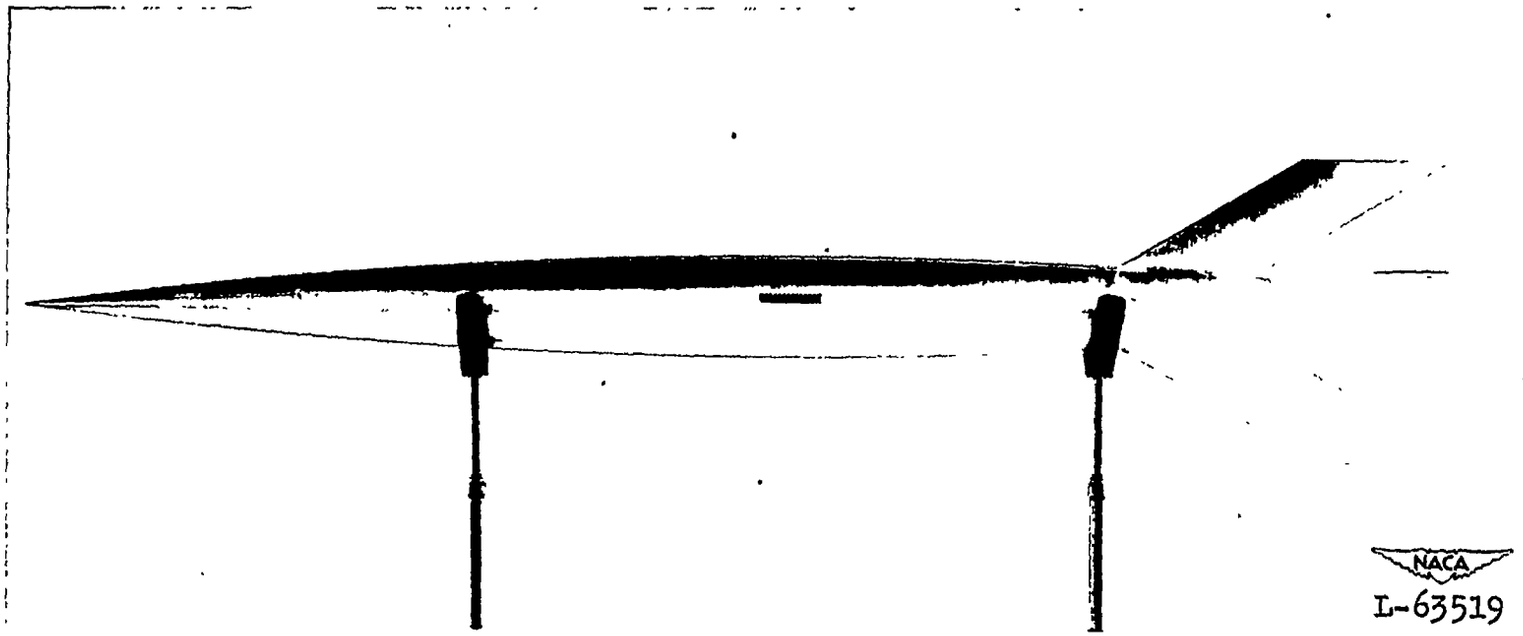

Figure 2.- Full-scale RM-10 test model.

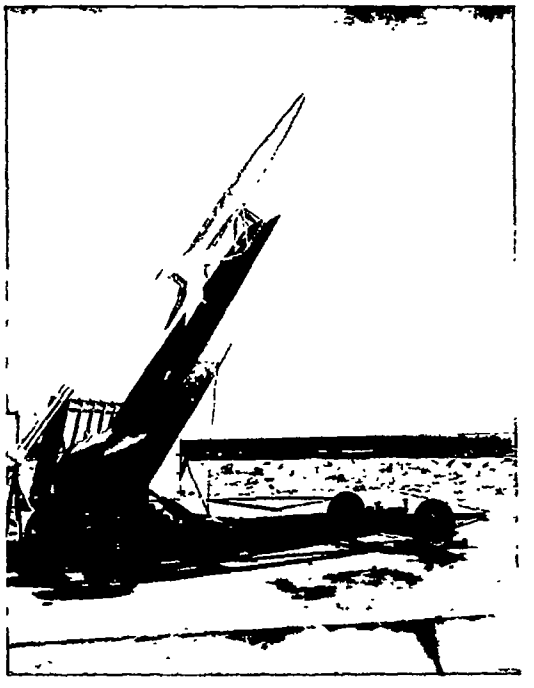

(a) Full-scale model.

NACA
L-60473

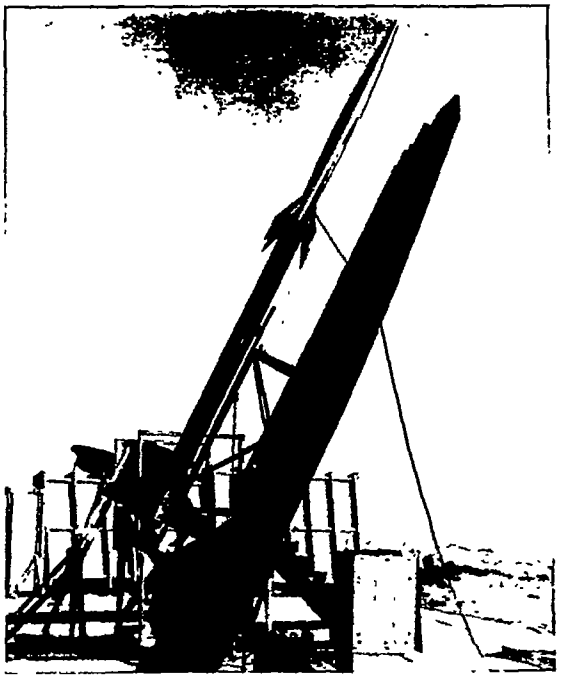

(b) Half-scale model with Deacon booster.

NACA
L-63870

Figure 3.- Views of models in launching position.

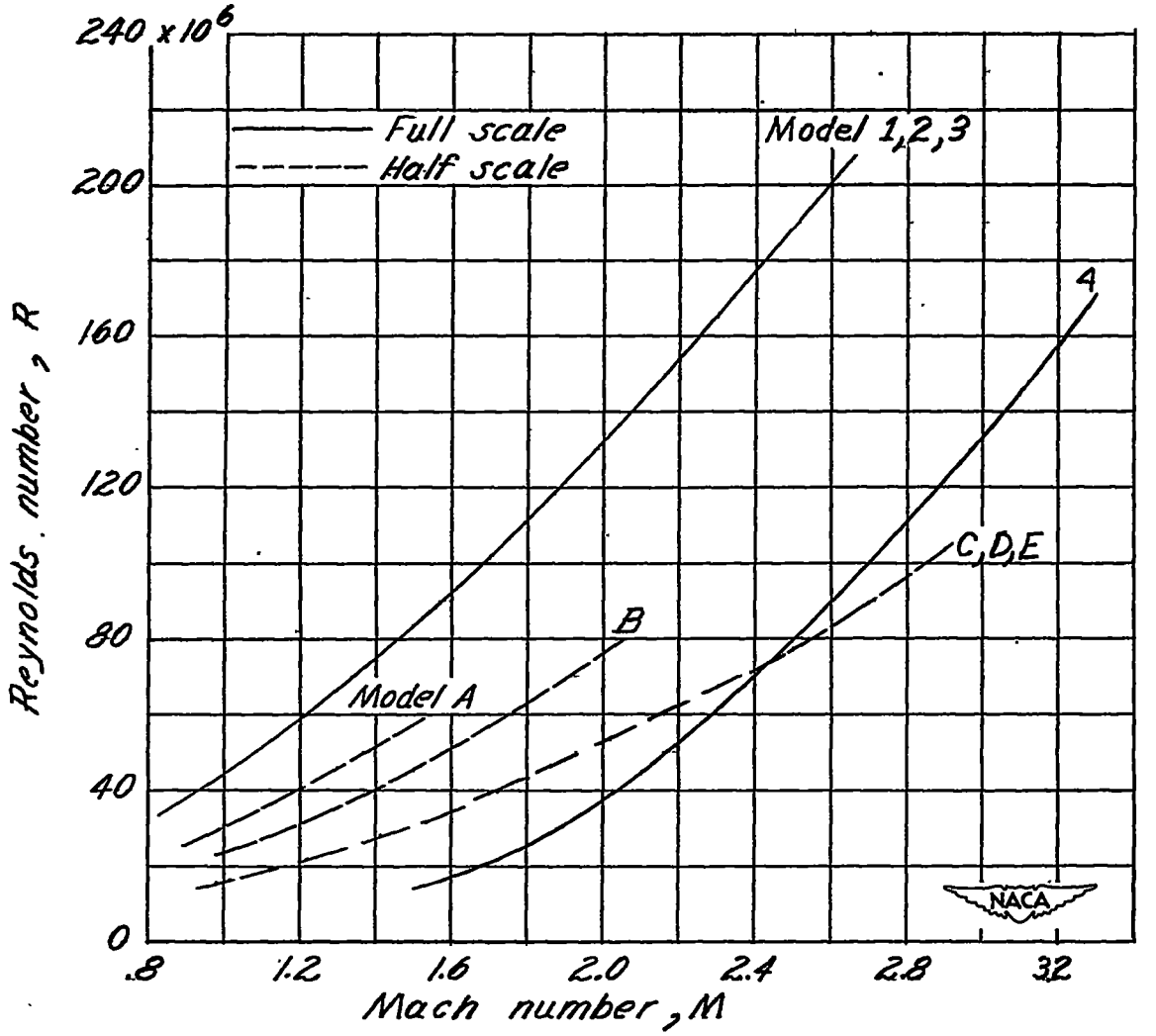

Figure 4.- Variation of Reynolds number with Mach number for the test models.

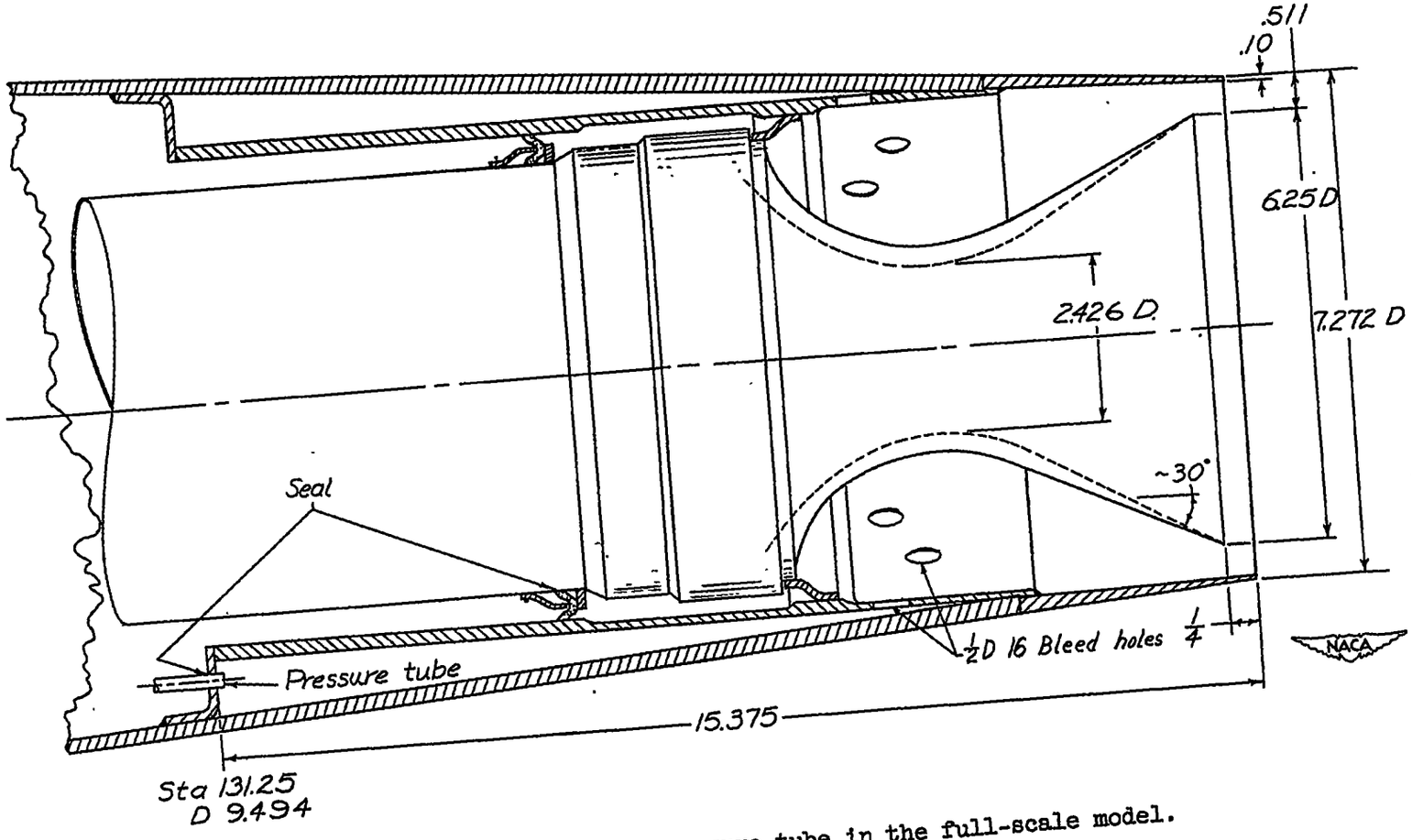

Figure 5.- Location of base-pressure tube in the full-scale model. Dimensions are in inches.

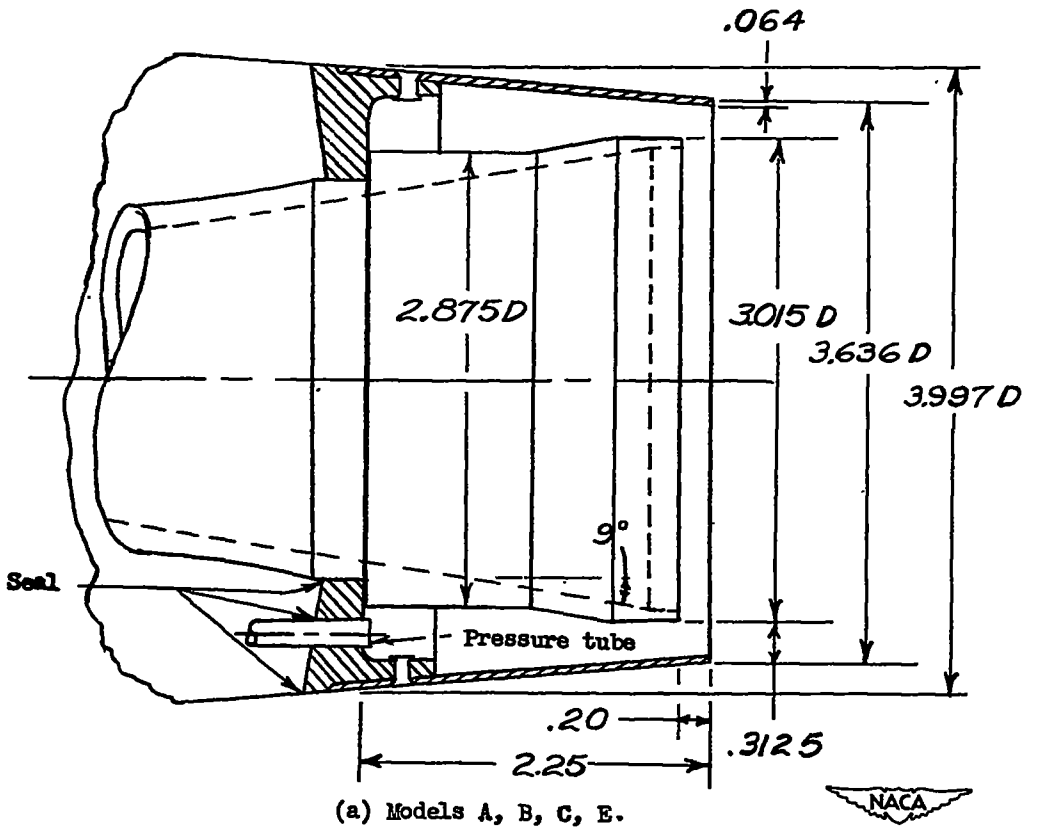

(a) Models A, B, C, E.

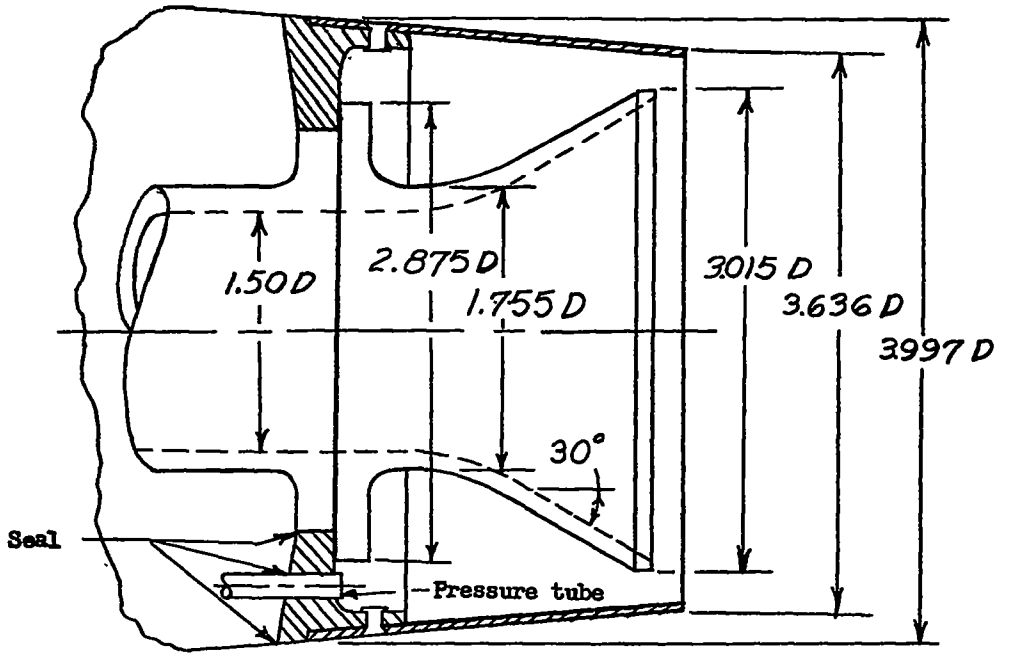

(b) Model D.

Figure 6.- Location of base-pressure tubes in the half-scale models. Dimensions are in inches.

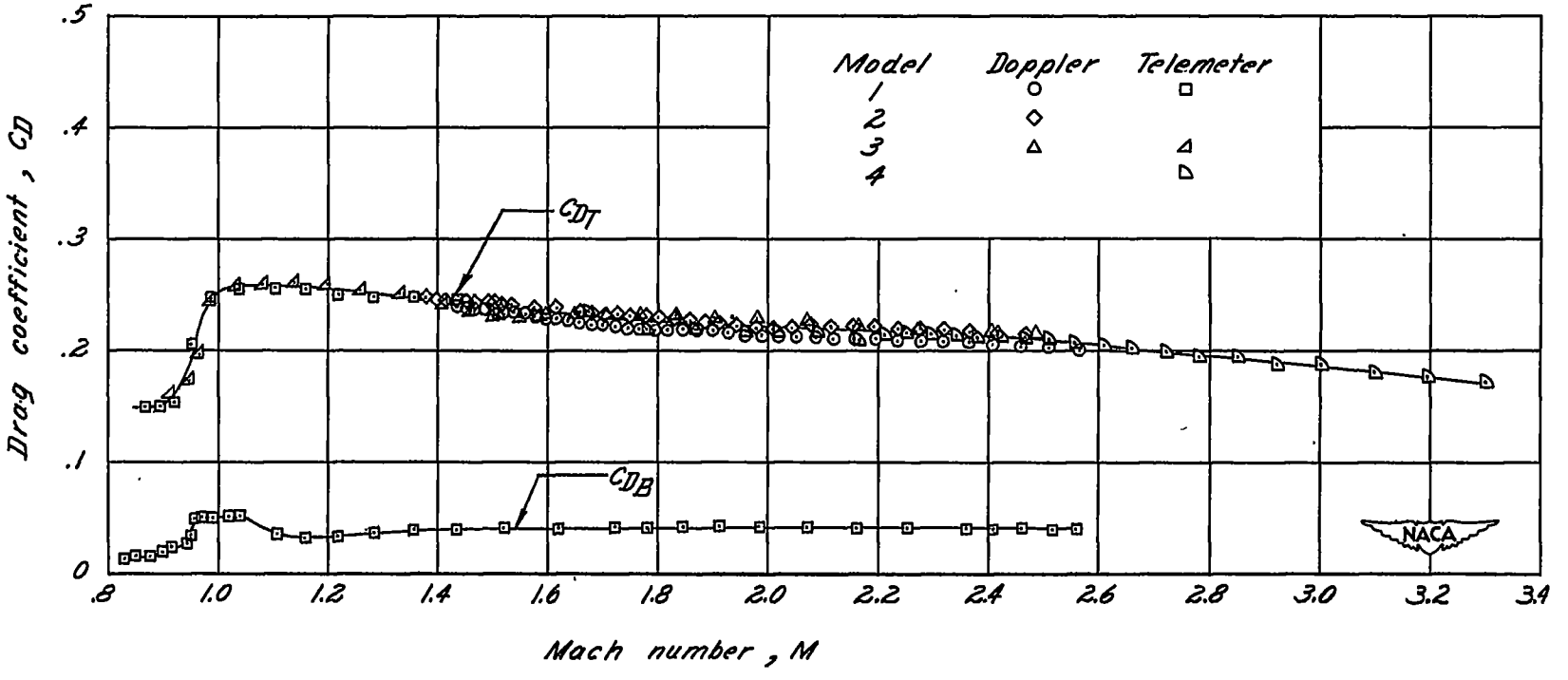

Figure 7.- Variation of total drag and base-drag coefficients with Mach number for the full-scale models. Drag coefficients based on body frontal area.

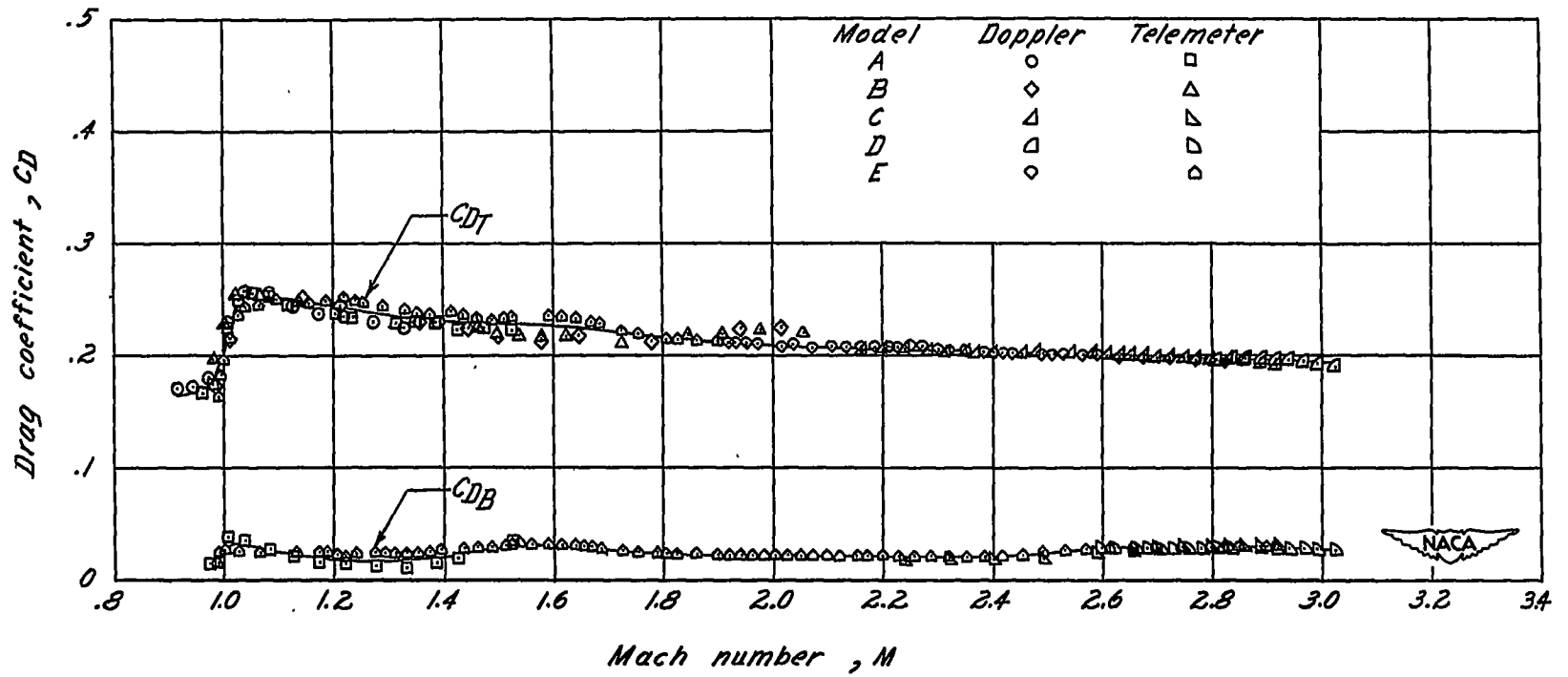

Figure 8.- Variation of total drag and base-drag coefficients with Mach number for the half-scale models. Drag coefficients based on body frontal area.

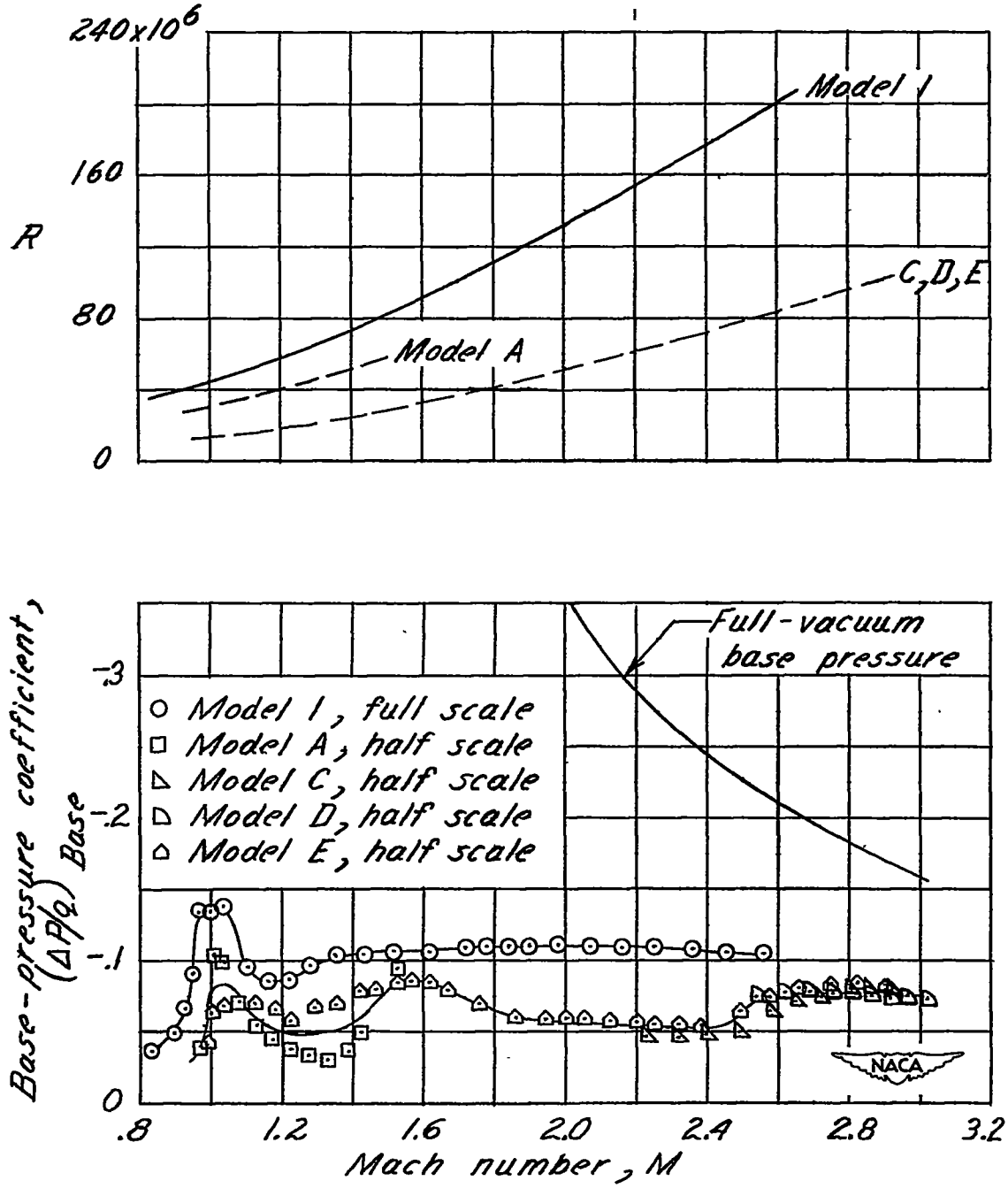

Figure 9.- Comparison of base-pressure coefficient for the full-scale and half-scale models with corresponding Reynolds number.

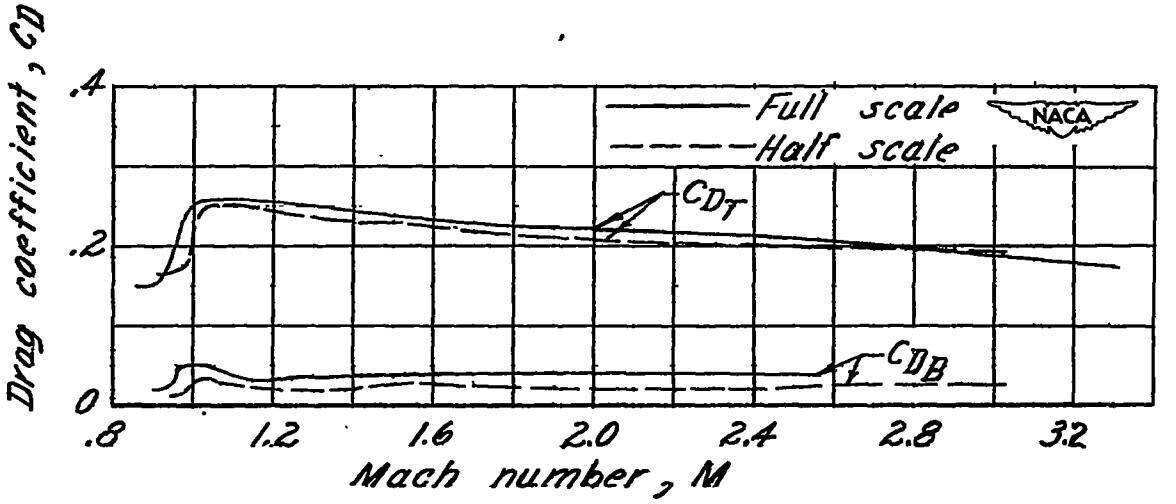

Figure 10.- Comparison of total drag and base-drag coefficients for the full-scale and half-scale models.

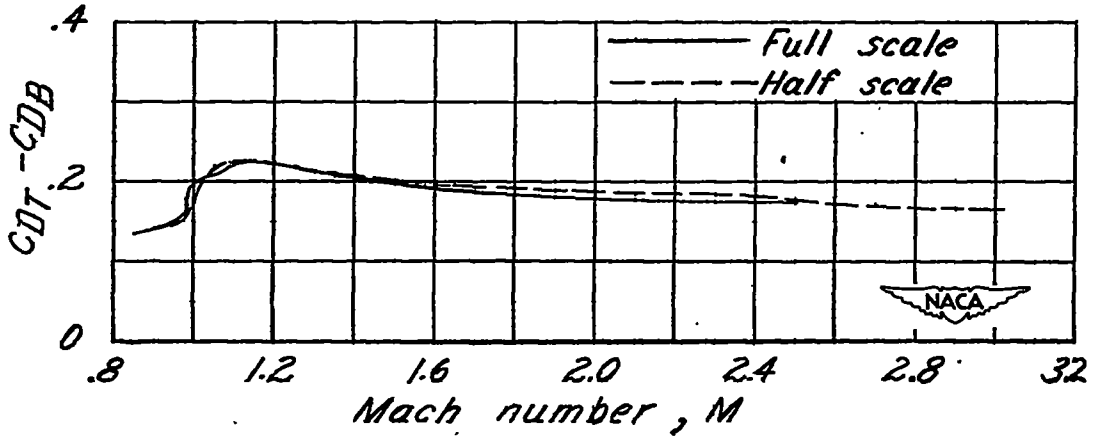

Figure 11.- Comparison of forebody drag coefficients for the full-scale and half-scale models.

NACA-Langley - 11-22-54 - 1000